

THROMBOSIS AND HEMOSTASIS

Control of VWF A2 domain stability and ADAMTS13 access to the scissile bond of full-length VWF

Christopher J. Lynch, David A. Lane, and Brenda M. Luken

Centre for Haematology, Department of Medicine, Imperial College London, London, United Kingdom

Key Points

- The vicinal disulphide bond and occupancy of its Ca²⁺-binding site cooperatively determine the stability of the VWF A2 domain.
- These 2 structural elements control the susceptibility of FL-VWF to proteolysis by ADAMTS13.

Rheological shear forces in the blood trigger von Willebrand factor (VWF) unfolding which exposes the Y1605-M1606 scissile bond within the VWF A2 domain for cleavage by ADAMTS13. The VWF A2 domain contains 2 structural features that provide it with stability: a vicinal disulphide bond and a Ca²⁺-binding site (CBS). We investigated how these 2 structural features interplay to determine stability and regulate the exposure of the scissile bond in full-length VWF. We have used differential scanning fluorimetry together with site-directed mutagenesis of residues involved in both the vicinal disulphide bond and the CBS to demonstrate that both of these sites contribute to stability against thermal unfolding of the isolated VWF A2 domain. Moreover, we show that the combination of site mutations can result in increased susceptibility of FL-VWF to proteolysis by ADAMTS13, even in the absence of an agent (such as urea) required to induce unfolding. These studies demonstrate that VWF A2 domain stability provided by its 2 structural elements (vicinal disulphide

bond and CBS) is a key protective determinant against FL-VWF cleavage by ADAMTS13. They suggest a 2-step mechanism for VWF A2 domain unfolding. (*Blood*. 2014;123(16):2585-2592)

Introduction

von Willebrand factor (VWF) is a multidomain protein, possibly the largest in blood. A mature VWF monomer (~250 kDa) is synthesized with domains in the order D'-D3-A1-A2-A3-D4-C1-C2-C3-C4-C5-C6-CK.¹ Following synthesis, VWF undergoes extensive posttranslational modification, including the formation of large multimers (500-20 000 kDa) through head-to-head and tail-to-tail disulphide bond formation between monomers.² VWF is either secreted directly, or packed into secretory vesicles termed Weibel-Palade bodies in endothelial cells or in α -granules of platelets and megakaryocytes. The structure of the VWF protein determines its functions. Its conformation undergoes changes during storage and secretion, under the rheological forces in the vasculature, and through interactions with other proteins. The VWF A2 domain plays important roles in VWF folding, in its unfolding for platelet capture, and in its proteolysis. Elements of the VWF A2 domain have been postulated to act as a shear bolt regulating the unfolding of the VWF molecule.³ During unfolding, multiple interaction sites for its protease, ADAMTS13, are exposed and the buried M1605-Y1606 scissile bond is made available.⁴ Proteolysis leads to a reduction in multimer size and downregulates platelet capture, thereby reducing its hemostatic potential.

The most notable structural specialization of the VWF A2 domain is the lack of a domain-spanning disulphide bond, a feature that is present between the N and C termini of the neighboring VWF A1 and A3 domains. To date, 3 different structures of the isolated VWF A2

domain have been determined by x-ray crystallography.^{3,5,6} The first structure of the VWF A2 domain established that the Y1605-M1606 scissile bond is indeed buried in the central core of the VWF A2 domain and therefore inaccessible to ADAMTS13.³ This corroborated previous findings that mechanical force (applied by shear flow⁷ or through atomic force microscopy⁸) or denaturing chaotropic agents⁹⁻¹¹ need to be applied for cleavage of full-length (FL) VWF to occur. A further structural differentiation of the VWF A2 domain in comparison with the homologous A domains is the lack of an α 4-helix; it contains instead a flexible "α4-less loop."³ Furthermore, crystal structure analysis showed the presence of a disulphide bond between the 2 vicinal cysteines, C1669-C1670, at the C terminus of the domain.^{3,12} The vicinal cysteines interacted with the hydrophobic core of the domain and with residues in close proximity to the scissile bond. We have previously shown that these vicinal cysteines form a disulphide bond which improves the thermostability of the VWF A2 domain and influence the interaction with, and susceptibility to cleavage by, ADAMTS13.¹³ Other features that may affect VWF A2 domain stability are a *cis* proline at position 1645³ and 2 N-linked glycosylation sites at N1515 and N1574 that have been found to influence cleavage by ADAMTS13.¹⁴

Additional crystal structures have revealed the coordination of a Ca²⁺ ion by a calcium-binding site (CBS) within the VWF A2 domain.^{5,6} The residues involved in Ca²⁺ coordination (D1596, R1597, A1600, N1602) lie in the α 3- β 4 loop, and toward the N

Submitted November 12, 2013; accepted February 16, 2014. Prepublished online as *Blood* First Edition paper, February 20, 2014; DOI 10.1182/blood-2013-11-538173.

The online version of this article contains a data supplement.

The publication costs of this article were defrayed in part by page charge payment. Therefore, and solely to indicate this fact, this article is hereby marked "advertisement" in accordance with 18 USC section 1734.

© 2014 by The American Society of Hematology

terminus of the domain in the $\beta 1$ sheet (D1498). Ca^{2+} has been shown to bind to and thermodynamically stabilize the VWF A2 structure in a concentration-dependent manner, with reported K_d ranging from $0.2\mu\text{M}$ to $3.8\mu\text{M}$.^{5,15} Mutagenesis of these residues that coordinate Ca^{2+} through their R groups (D1498, D1596, N1602) has been shown to prevent the interaction of the Ca^{2+} ion with the VWF A2 domain.^{5,6} The VWF A2 D1498A⁶ and N1602A⁵ VWF A2 domain mutants have been found to elicit an increase in susceptibility to proteolysis by ADAMTS13.

These previous studies have highlighted the importance of both the vicinal disulphide bond and the CBS on the structure and stability of the isolated VWF A2 domain. In this report, we investigate how these structural features act together to maintain the structural integrity of the VWF A2 domain and protect against proteolysis of FL-VWF by ADAMTS13.

Methods

Recombinant VWF protein expression

The recombinant VWF A2 domain fragments, VWF A2VicCC (amino acids 1473-1670) and VWF A2 Δ CC (1473-1668), with a C-terminal myc/his tag, were expressed in HEK293 EBNA cells. Mutations D1498A, D1596A, N1602A, and combinations thereof were introduced using KOD polymerase (EMD Millipore), a recombinant form of *Thermococcus kodakaraensis* KOD1 DNA polymerase, according to the manufacturer's instructions for site-directed mutagenesis. These mutations were also introduced into pcDNA3.1-VWF¹⁴ and pcDNA3.1-VWFA2¹³; FL-VWF and its variants were then expressed in HEK293 cells.

VWF A2 detection and characterization

After 3 days the medium from transiently transfected HEK293 EBNA cells was harvested and the cells lysed with phosphate-buffered saline (PBS) 1% igepal. The medium and lysate were run on 4% to 12% Bis-Tris gels and the VWF A2 domain protein detected on western blot with an antibody against the C-terminal myc tag. For further experiments, the VWF A2 proteins were purified by Ni^{2+} chromatography and quantified by bicinchoninic acid assay as previously described.¹³ Purified VWFA2 domains A2 Δ CC and A2VicCC, $50\mu\text{L}$ of 0.5 mg/mL , were characterized by size-exclusion high-performance liquid chromatography (SE-HPLC) by applying to a Polyhydroxyethyl A 300 \AA column (PolyLC, Inc.) at a flow rate of 0.25 mL/minute in $50\text{ mM KH}_2\text{PO}_4$, 100 mM NaCl , pH 7.8. A $10\times$ dilution of gel-filtration standards (Bio-Rad) was used to calibrate the column.

Differential scanning fluorimetry

During differential scanning fluorimetry (DSF), the environmentally sensitive dye SyproOrange interacts with previously hidden hydrophobic regions upon temperature-induced unfolding, thereby increasing the fluorescence (FU) intensity and providing a quantitative measure of the fraction of protein in its unfolded state. After the protein has fully unfolded, it starts to aggregate causing a reduction in the FU signal.¹⁶ Purified VWF A2 domain variants were dialyzed into 20 mM Tris (pH 7.8), 50 mM NaCl , and protein quantified by bicinchoninic acid assay (Pierce; Thermo Scientific). Samples contained $1.5\mu\text{g}$ of purified VWF A2 domain, $5\times$ SyproOrange dye (Sigma-Aldrich), 1 mM EDTA or 5 mM CaCl_2 in 20 mM Tris (pH 7.8), 50 mM NaCl in a total volume of $60\mu\text{L}$. FU increase brought about by unfolding of the VWF A2 domain was monitored by high-resolution melting analysis (HRM) using Rotor-Gene Q real-time polymerase chain reaction (PCR) instrument (Qiagen). Assays were performed over a temperature range of 25°C to 80°C using a ramp of 1°C min^{-1} in steps of 1°C . Samples were investigated in at least 3 independent experiments and FU values individually baseline corrected. The initial FU value at 25°C was regarded as 0% of the maximal FUs measured and

the maximal fluorescence value as 100%. The transition midpoint (T_m), that is, 50% unfolded protein, of the unfolding curve was calculated using the Boltzmann equation (analyzed with GraphPad Prism).

FL-VWF quantification and multimer analysis

Medium from transiently transfected HEK293 cells expressing FL-VWF and its variants was collected after 3 days. Levels of VWF antigen (VWF:Ag) in the medium and lysate were determined by VWF enzyme-linked immunosorbent assay (ELISA) using polyclonal antibodies for immobilization and detection (Dako), as previously described.¹⁴ Expression media was collected and concentrated 10-fold using Ultracel 100-kDa cutoff spin filters (Millipore) and dialyzed into 20 mM Tris (pH 7.8), 50 mM NaCl . Fifty nanograms of each VWF variant was electrophoresed on a 2% high gelling temperature agarose for protein (Lonza) gel and western blots probed with anti-VWF-horseradish peroxidase (HRP) polyclonal antibody (Dako) to assess VWF multimer formation.

ADAMTS13 proteolysis of FL-VWF and its variants

Recombinant ADAMTS13 with a C-terminal myc/his tag was stably expressed in HEK293 cells, as previously described.¹³ The FL-VWF and its variants as well as ADAMTS13 were separately preincubated in 20 mM Tris (pH 7.8), 50 mM NaCl , $5\text{ mM CaCl}_2 \pm 1.5\text{ M urea}$ at 37°C for 45 minutes. FL-VWF and ADAMTS13 were then combined at a final concentration of 1 or $7\mu\text{g/mL}$ VWF and 5 nM ADAMTS13 , and incubated at 37°C for proteolysis to occur. Reactions were stopped after 15 and 180 minutes by the addition of EDTA. To determine proteolysis, 5% 2-mercaptoethanol/sodium dodecyl sulfate was added to reduce the FL-VWF and its variants. The samples were then run on 3% to 8% Tris-acetate gels (Invitrogen) and VWF bands detected on western blot using polyclonal anti-VWF antibody (Dako).

To analyze changes in collagen-binding ability induced by proteolysis with ADAMTS13, VWF:collagen binding assay (CBA) was performed in independent experiments. Collagen type III ($10\mu\text{g}$) from human placenta (Sigma-Aldrich) was coated onto Immulon 4HBX plate (Nunc). After sample incubation and washing, bound VWF was detected using polyclonal HRP-linked VWF antibody (Dako). Collagen binding was compared with standards from a commercial VWF:CBA ELISA (Technoclone) and divided by simultaneously determined VWF antigen levels to calculate the VWF: CBA/VWF:Ag ratio.

Results

The vicinal disulphide bond and binding of Ca^{2+} cooperate to stabilize the VWF A2 domain

A structure of the VWF A2 domain depicting its 3 key features, its vicinal disulphide bond, its CBS, and the buried Y1605-M1606 scissile bond is shown in Figure 1A. To assess the role of the vicinal disulphide bond on the stability of the VWF A2 domain, we expressed and purified the VWF A2 domain containing these cysteines, A2VicCC (M1473-C1670), and without them, A2 Δ CC (M1473-R1668). Using SE-HPLC, it was shown that these purified fragments formed monomers of expected molecular weight and free from aggregates (see supplemental Figure, available on the *Blood* Web site).

These purified A2 domains were subjected to DSF assays to evaluate stability to thermal unfolding. The temperature-induced unfolding curves of the purified VWF A2 domains are shown in Figure 1B over a temperature range from 25°C to 80°C . The A2 Δ CC domain fragment showed an increase and then decrease in FU, with a maximum between 40°C and 50°C . There was clear evidence of uncooperative unfolding of this fragment, shown by the inflection on the upward part of the curve (discussed below in the context of

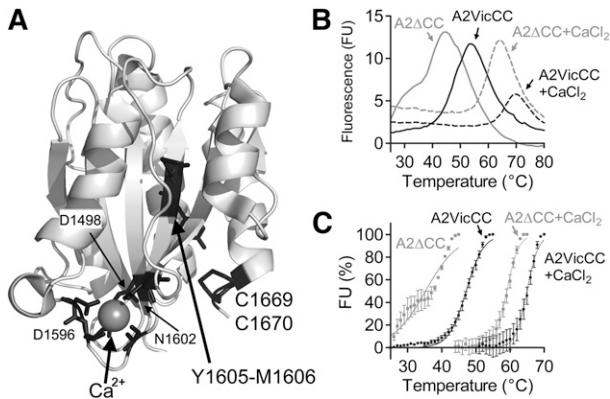


Figure 1. Structure and thermodynamic unfolding of the VWF A2 domain. (A) Crystal structure of the VWF A2 domain (PDB 3ZQK, modified in Pymol) is shown with the vicinal disulphide bond (C1669, C1670), scissile bond (Y1605, M1606), and Ca²⁺-coordinating residues in black. (B) DSF measurements using the dye SyproOrange were taken at 510 nm every 1°C, with a ramp 1°C min⁻¹, over a temperature range of 25°C to 80°C. FU reads were individually baseline corrected to a buffer only control with EDTA or CaCl₂. Representative curves of the VWF A2 domain constructs A2VicCC and A2ΔCC in the presence of an excess of 5 mM CaCl₂ or 1 mM EDTA to chelate-free Ca²⁺ are shown. (C) The unfolding curves were normalized, the lowest FU value was assigned as 0% and the highest FU value represents 100%. Resultant curves were fitted using the sigmoidal Boltzmann equation in Graphpad and the transition midpoint (T_m) calculated, see Table 1. Results are means of at least 3 independent experiments ± standard error of the mean (SEM).

Figure 1C). The VWF A2 domain demonstrates increasing stability to increasing temperature when the vicinal disulphide bond is introduced (in the A2VicCC fragment) and when Ca²⁺ is present (A2ΔCC + CaCl₂). The most stable A2VicCC construct in 5 mM CaCl₂ demonstrates a smaller change in FU in its unfolding transition (Figure 1A), this could be attributed to the reduced efficiency of the SyproOrange dye at higher temperatures (data not shown). To better analyze the DSF results, unfolding curves were buffer corrected and the lowest FU value was normalized to 0% and the maximal FU value normalized to represent 100% of unfolding (Figure 1C). Sigmoidal unfolding curves characteristic of cooperative unfolding were then fitted to the Boltzmann equation and transition midpoints, T_m, derived. From the unfolding curves and T_m of A2VicCC in the presence of EDTA or CaCl₂ (Figure 1C; Table 1), the importance of Ca²⁺ stabilization can be readily seen by a 17.9°C shift in T_m from 47.1°C ± 0.10°C to 65.0°C ± 0.22°C. In the absence of the vicinal cysteines (A2ΔCC), a 23.9°C shift in T_m from 35.2°C ± 0.38°C to 59.1°C ± 0.17°C can be observed upon addition of Ca²⁺. The curve of the A2ΔCC domain fragment displayed some uncooperative unfolding (Figure 1C). This was further corroborated by our finding that the A2ΔCC fragment showed signs of some aggregation by SE-HPLC when incubated for 10 minutes at 40°C in the presence of EDTA (see supplemental Figure). We have previously shown that the vicinal cysteines stabilize the VWF A2 domain through disulphide bond formation.¹³ The introduction of the vicinal cysteines alone caused a shift in T_m of 11.9°C in the absence of Ca²⁺ (compare A2ΔCC + EDTA, 35.2°C ± 0.38°C, to A2VicCC + EDTA, 47.1°C ± 0.10°C) and a smaller shift of 5.9°C in the presence of Ca²⁺ (compare A2ΔCC + CaCl₂, 59.1°C ± 0.17°C, to A2VicCC + CaCl₂, 65.0°C ± 0.22°C). Thus, we show that both vicinal disulphide bond formation and the binding of Ca²⁺ separately stabilize the VWF A2 domain. It is also evident that these structural features have an additive effect, as the VWF A2 domain is most stable when both of these features are imparting their effects (A2VicCC + CaCl₂, T_m 65.0°C ± 0.22°C) and least

stable when both of these features are absent (A2ΔCC + EDTA, T_m 35.2°C ± 0.38°C).

Mutation of the VWF A2 domain Ca²⁺-binding residues influences secretion and thermostability

To further define the relationship between the vicinal disulphide bond and the CBS, the 3 residues that coordinate Ca²⁺ through their R groups, D1498, D1596, and N1602, were mutated to alanine. Mutations were introduced as single point and combination mutations into A2VicCC and A2ΔCC. All A2VicCC domain variants were expressed and secreted by HEK293EBNA cells with similar efficiency to wild-type (WT) A2VicCC. Variants were purified and protein stability analyzed using DSF. As expected, the addition of Ca²⁺ had a minimal effect on the thermostability of these variants (Figure 2A-C; Table 1), suggesting that Ca²⁺ coordination has been ablated by the mutations. Nevertheless, the mutations can be divided into 2 distinct groups. The A2VicCC D1498A and A2VicCC N1602A variants had similar stabilities (T_m 49.7°C ± 0.05°C and 48.1°C ± 0.05°C, respectively) to that of WT A2VicCC in the absence of Ca²⁺ (A2VicCC + EDTA, T_m 47.1°C ± 0.10°C), indicating “destabilization” of the VWF A2 domain by the mutations. The A2VicCC D1596A variant, however, had similar stability (T_m 62.1°C ± 0.14°C) to that of the WT A2VicCC in the presence of Ca²⁺ (A2VicCC + CaCl₂, T_m 65.0°C ± 0.22°C), indicating “stabilization” of the CBS, even in the absence of Ca²⁺. All of the combination mutants containing D1498A resulted in the destabilization of VWF A2 domain (Figure 2D-E,G), with the mutants having a T_m ~50°C. However, the “stabilizing” D1596A mutation in combination with the “destabilizing” N1602A mutation resulted in a “stabilized” A2VicCC D1596/N1602A variant (T_m 60.6°C ± 0.08°C) (Figure 2F; Table 1).

When the CBS mutations were introduced into A2ΔCC, only the D1596A and D1596A/N1602A substitutions (that had shown a stabilizing effect on A2VicCC) were expressed and secreted (Figure 3A upper panel). In contrast, all the variants were secreted when introduced into A2VicCC (Figure 3A, lower panel). When the destabilizing mutations (D1498A, N1602A, D1498A/D1596A, D1498A/N1602A, and D1498A/D1596A/N1602A) were introduced into A2ΔCC, no protein was detected in the medium, while it was clearly visible in the cell lysate (Figure 3A, upper panel). This again indicates the importance of both the vicinal cysteines and the CBS for domain stability. For the stabilizing mutations (D1596A and D1596A/N1602A), a doublet band was observed in the lysate. The faster moving band represents an unglycosylated intermediate,

Table 1. T_m of VWF A2VicCC and A2ΔCC variants as determined by DSF

	T _m , °C			
	A2VicCC		A2ΔCC	
	1 mM EDTA	5 mM CaCl ₂	1 mM EDTA	5 mM CaCl ₂
WT	47.1 ± 0.10	65.0 ± 0.22	35.2 ± 0.38	59.1 ± 0.17
D1498A	49.7 ± 0.05	49.6 ± 0.06	N/A	N/A
D1596A	62.1 ± 0.14	62.5 ± 0.16	55.5 ± 0.06	56.1 ± 0.08
N1602A	48.1 ± 0.05	50.3 ± 0.09	N/A	N/A
D1498A/D1596A	51.3 ± 0.07	50.6 ± 0.06	N/A	N/A
D1498A/N1602A	49.7 ± 0.07	49.1 ± 0.05	N/A	N/A
D1596A/N1602A	60.6 ± 0.08	61.6 ± 0.05	54.6 ± 0.06	54.9 ± 0.06
D1498A/D1596A/N1602A	50.6 ± 0.06	49.8 ± 0.06	N/A	N/A

Results are presented as mean ± SEM derived from at least 3 independent experiments. N/A, not assessed.

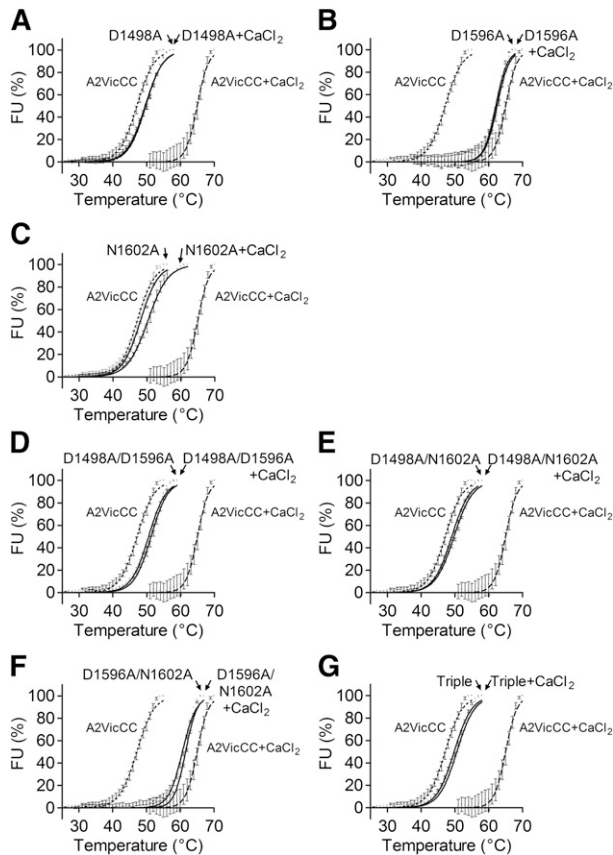


Figure 2. Mutagenesis of Ca^{2+} -coordinating residues abolishes the stabilizing effect of Ca^{2+} in A2VicCC. DSF measurements were carried out in the presence of 5 mM CaCl_2 (black) or 1 mM EDTA (gray) with the WT A2VicCC construct and Ca^{2+} -binding site mutants D1498A (A), D1596A (B), N1602A (C), D1498A/D1596A (D), D1498A/N1602A (E), D1596A/N1602A (F), and D1498A/D1596A/N1602A (triple, G). Results are means \pm SEM of at least 3 independent experiments.

confirmed by EndoH_f digestion (data not shown). The expressed A2 Δ CC D1596A and D1596A/N1602A variants were purified and DSF assays performed (Figure 3B-C). Again, the thermostability of these variants was not influenced by the presence or absence of Ca^{2+} (Table 1). Notably, these variants had a similar stability to WT A2 Δ CC + CaCl_2 , with $T_m \sim 55^\circ\text{C}$.

FL-VWF proteolysis by ADAMTS13 is controlled by the CBS and vicinal disulphide bond

To study the effects of the vicinal cysteines and the CBS beyond the context of the isolated VWF A2 domain, mutations D1498A, D1596A, and N1602A were introduced into FL-VWF and the previously described variant FL-VWFFicGG, in which both the vicinal cysteines (C1669-C1670) were substituted with glycine, to prevent vicinal disulphide bond formation. To assess the effect of each of these introduced mutations on FL-VWF secretion and multimer formation, the FL-VWF variants were transiently transfected into HEK cells, which have been shown to store recombinant VWF in pseudo Weibel-Palade bodies.¹⁷ No statistically significant differences in VWF Ag levels of WT and variants of FL-VWF and FL-VWFFicGG in medium and lysate were observed (data not shown). FL-VWF multimer analysis revealed some loss of the highest molecular weight multimers for variants FL-VWF VicGG D1498A and VicGG N1602A (Figure 4A). These destabilized variants may have been intracellularly retained or may have been

somewhat more prone to degradation by intracellular/extracellular proteases.

Proteolysis assays with 5nM ADAMTS13 were performed in which the FL-VWF variants were incubated in the presence and absence of 1.5 M urea. Proteolysis reactions were terminated after 15 minutes and 3 hours, and samples reduced and cleavage products detected on western blot (Figure 4B). Under these particular conditions where there was no detectable cleavage of WT FL-VWF, even when urea was added for unfolding, there was also no cleavage of the FL-VWF D1596A variant (Figure 4B, upper panel). However, the FL-VWF D1498A and N1602A variants could be partially cleaved after prolonged (3 hours) incubation in the presence of urea. The FL-VWF VicGG variant could also be cleaved in urea: the addition of the D1596A mutation did not protect against this, as expected (Figure 4B, lower panel). What was most striking was the rapid cleavage of the FL-VWF GG variant when the D1498A and N1602A mutations were also introduced (Figure 4B, lower panel). These 2 composite variants were almost completely cleaved after 3 hours, regardless of whether urea was added for unfolding.

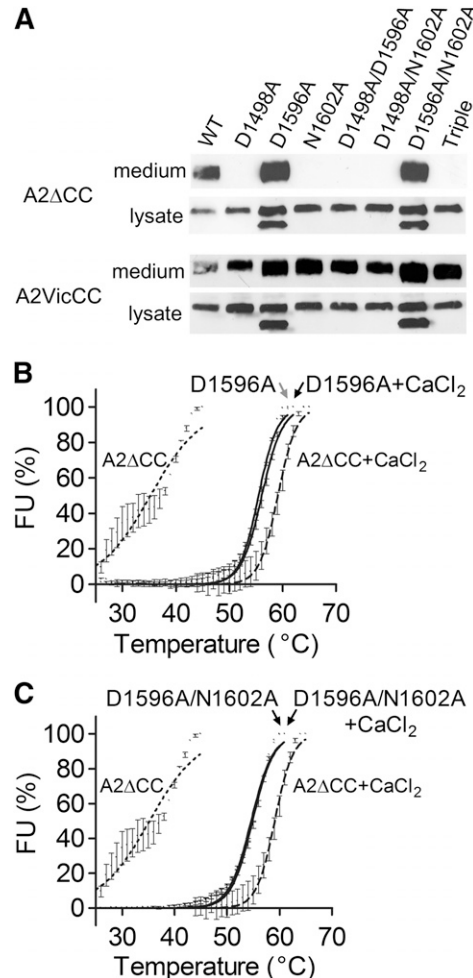
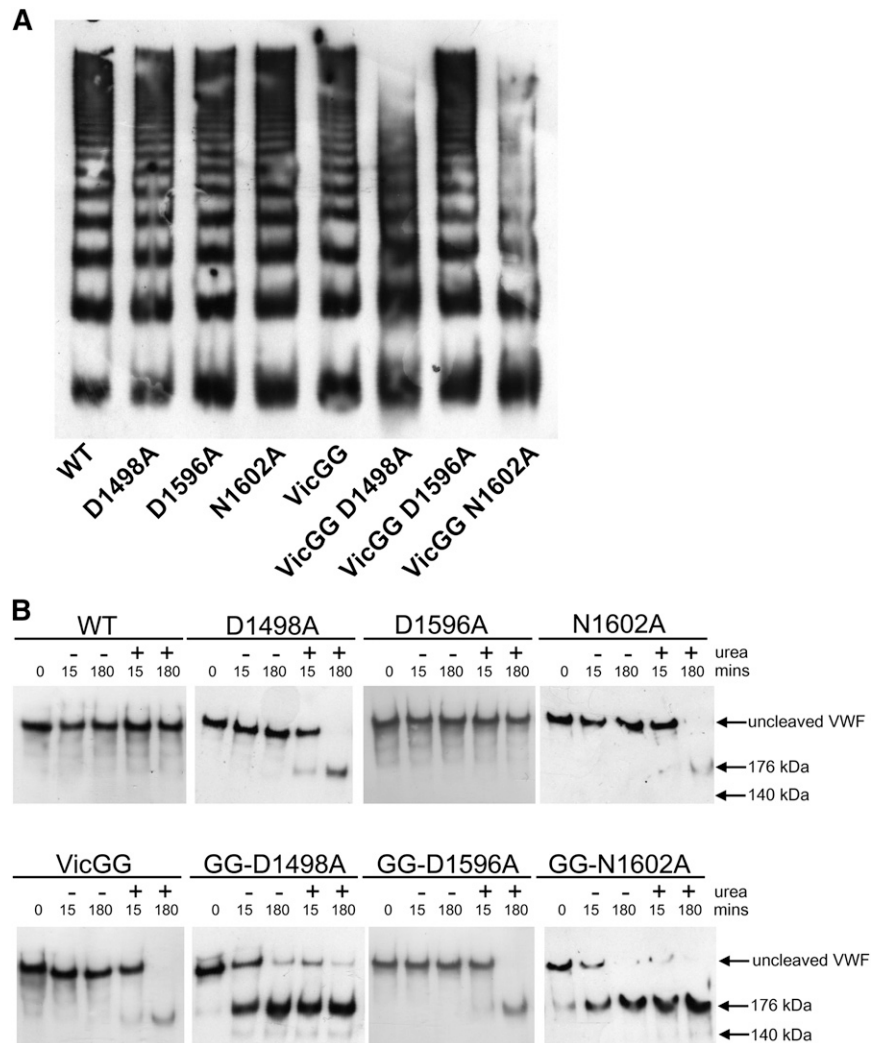


Figure 3. Expression and thermostability of the Ca^{2+} -binding site mutants in A2 Δ CC. (A) VWF A2 domain fragments with (A2VicCC) and without (A2 Δ CC) the vicinal cysteines were transiently expressed in HEK293EBNA cells. After 3 days, the medium was collected and the cells lysed with PBS 1% igepal and vigorous pipetting. After centrifugation to remove cell debris, the medium and lysate were run on 4% to 12% Bis-Tris gels and the VWF A2 domain protein detected on western blot with an antibody against the C-terminal myc tag. (B-C) The successfully secreted A2 Δ CC WT and Ca^{2+} mutants were subsequently purified and subjected to DSF analysis. Results are means \pm SEM of at least 3 independent experiments.

Figure 4. Characterization and proteolysis of the vicinal cysteine and Ca²⁺ variants in FL-VWF. FL-VWF containing single-point mutations of the Ca²⁺-binding residues, alone or in combination with mutation of the vicinal cysteines to glycines (VWF-VicGG), were expressed in HEK293 cells. (A) Multimer formation was analyzed on a 1.4% agarose gel and VWF bands detected on western blot with anti-VWF polyclonal antibody to determine the multimer composition of the FL-VWF variants. (B) Proteolysis of FL-VWF by ADAMTS13. The VWF variants and ADAMTS13 were separately preincubated in 20 mM Tris (pH 7.8), 50 mM NaCl, 5 mM CaCl₂ ± 1.5 M urea at 37°C for 45 minutes. VWF (1 μg/mL) and ADAMTS13 (5 nM) were then combined, incubated at 37°C and reactions stopped after 15 minutes and 180 minutes by the addition of EDTA. VWF cleavage products were resolved after reduction with 2-mercaptoethanol. The samples were run on a 3% to 8% Tris-acetate gel and VWF bands on western blot detected using anti-VWF antibody.



In separate experiments, the consequences of incubation with ADAMTS13 on collagen binding of the FL-VWF variants was explored. We found that VWF:CBA/VWF:Ag ratio varied between different transfections and have therefore set VWF:CBA/VWF:Ag at time point 0 at 100%. In the selected conditions, up to 3 hours' incubation with ADAMTS13 did not alter CBA of WT FL-VWF or FL-VWF D1596A (Figure 5A). The 2 FL-VWF N1602A and D1498A variants did, however, lose some ability to bind collagen after 3 hours' incubation. Addition of urea with ADAMTS13 accelerated loss of collagen binding of WT FL-VWF following incubation and the FL-VWF N1602A and D1498A variants, the latter exhibiting ablated collagen binding at 3 hours (Figure 5B). In contrast, the FL-VWF D1596A variant retained its collagen-binding ability in the presence of urea (Figure 5B).

When ADAMTS13 was incubated with FL-VWF VicGG, a modest reduction of collagen binding was observed (Figure 5C). This variant was not stabilized by introduction of the D1596A mutation. However, introduction of the N1602A and D1498A mutations into FL-VWF VicGG resulted in near complete loss of CBA, even in the absence of urea as an unfolding agent (Figure 5C). Predictably, addition of urea to these FL-VWF VicGG variants also resulted in almost complete loss of collagen binding (Figure 5D).

Discussion

The vicinal disulphide bonds between C1669-C1670 and the Ca²⁺-coordination site are about 13 Å apart in the 3ZQK crystal structure and both located at what is often depicted as the "bottom" of the VWF A2 domain. We present the first study of their functional interplay. We have found using DSF and thermal-induced unfolding that both are separate determinants of the stability of the VWF A2 domain. Disruption of either of these 2 structural features does not preclude a role in stability of the other. However, we did also observe a synergistic effect: while Ca²⁺ binding causes an 17.9°C increase in T_m when the vicinal disulphide bond is present (very similar to the 19°C shift in T_m reported previously⁵), we found that the stabilizing effect of Ca²⁺ was much larger in the absence of the vicinal disulphide bond, with a 23.9°C increase in T_m. Interestingly, the VWF A2 domain without both stabilizing features becomes so unstable that it no longer displays characteristic cooperative unfolding.

As well as probing the structural stability of the VWF A2 domain by addition and removal of Ca²⁺, we also studied the influence of individual residues that coordinate Ca²⁺ through their R group. We did this by their mutation to alanine, in the presence (with A2VicCC) and in the absence (with A2ΔCC) of the vicinal disulphide bond.

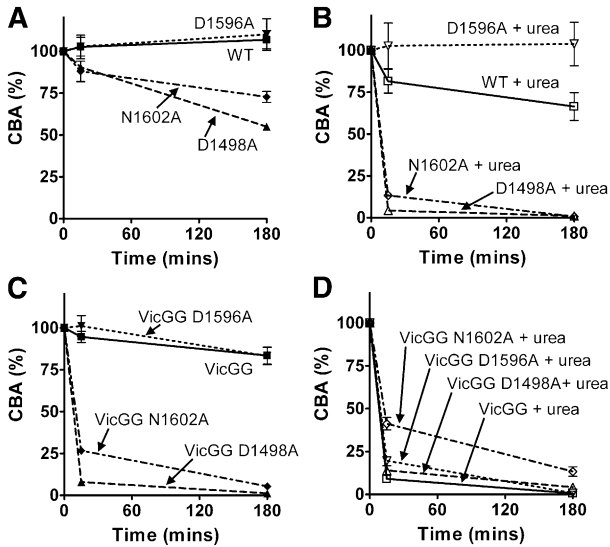


Figure 5. Detection of proteolysis of FL-VWF variants by collagen-binding assay. (A-D) The VWF variants and ADAMTS13 were separately preincubated in 20 mM Tris (pH 7.8), 50 mM NaCl, 5 mM CaCl₂ ± 1.5 M urea at 37°C for 45 minutes. VWF (1 μg/mL) and ADAMTS13 (5 nM) were then combined, incubated at 37°C, and reactions stopped after 15 minutes and 180 minutes by the addition of EDTA. To analyze the extent of proteolysis, CBA was determined. For each FL-VWF variant the VWF:CBA/VWF:Ag ratio at both time points was normalized against the ratio determined at the start of the assay (100%). VWF concentrations in assays with urea (B,D) contained 7 μg/mL VWF, hence samples could be diluted further and urea no longer interfered with the assay. Results are means ± SEM from 3 independent analyses.

The A2VicCC D1498A and N1602A domain variants were no longer stabilized upon addition of Ca²⁺, while the mutant with D1596A displayed enhanced stability even in the absence of Ca²⁺. These findings are in good agreement with published results by Jakobi et al, although the D1498A mutant was not secreted in their study and could therefore not be investigated.⁵ The stabilizing effect

of mutation D1596A has been explained by a reduction in electrostatic repulsion otherwise seen between residues D1596 and D1498 in the absence of Ca²⁺.⁵ It has been shown that binding of Ca²⁺ moves the D1596 residue by >16 Å.⁶ This appears to confer the increase in structural stability by reducing the B factor of the α3β4 loop and increasing the strength of the interaction between the β1 and β4 sheets.^{5,6} The combination of introducing mutation D1498A or N1602A together with simultaneous deletion of the vicinal cysteines produced a major reduction in the structural stability, as the resulting VWF A2 domain mutants were no longer secreted. Again, stability of the VWF A2 domain fragment was enhanced by introduction of the D1596A and the D1596A/N1602A combination mutations, even in the absence of Ca²⁺.

The conformational response of the VWF A2 domain to mechanical force has been studied at the molecular level by techniques involving force induced unfolding and optical tweezers.^{5,8,15,18} These studies have all been performed with VWF A2 containing the vicinal cysteines, although it was not established whether the vicinal disulphide bond was correctly formed, even when redox chemistry was used to attach DNA handles to the VWF A2 protein.⁸ The force induced unfolding studies have been instrumental to demonstrate how Ca²⁺ stabilizes the VWF A2 domain and protects against cleavage by ADAMTS13.^{5,15} Nevertheless, some conceptual differences also became apparent and conflicting evidence has been published on whether Ca²⁺ protects against the unfolding of the VWF A2 domain,⁵ or rather enhances its refolding,¹⁵ thereby decreasing the time window for ADAMTS13 to cleave VWF. Another disparity in the optical tweezer studies is the existence of an unfolding intermediate. Auton et al had previously described an unfolding intermediate in a solution unfolding experiment using urea.⁹ In 2 of 3 optical tweezer experiments with the VWF A2 domain an intermediate has been detected.^{5,8} The exact structure of the unfolding intermediate and whether it still comprises the β4 strand with the ADAMTS13 cleavage site remains to be determined as it is difficult to derive from contour

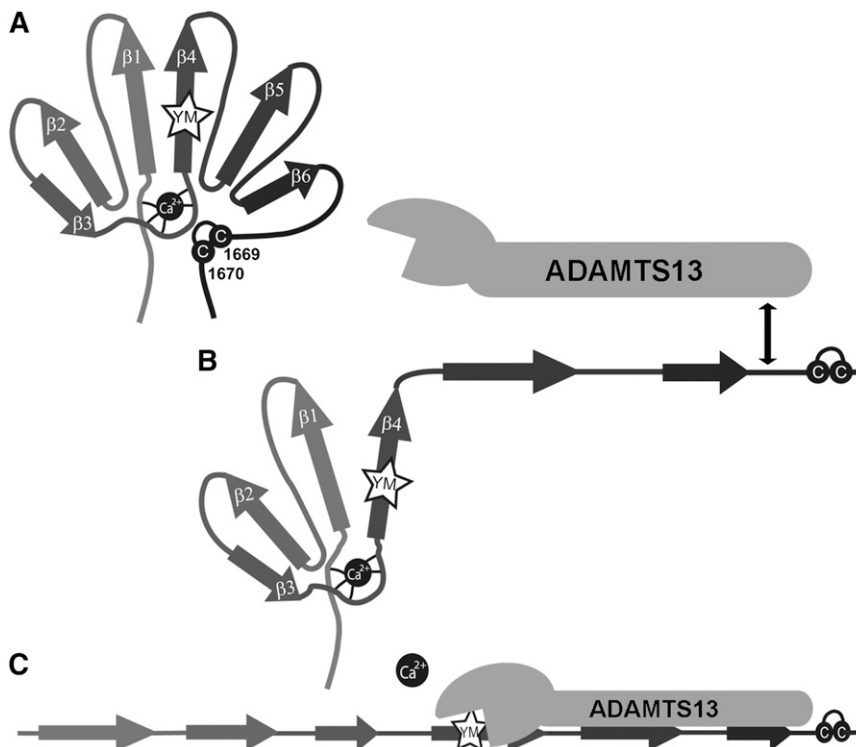


Figure 6. Unfolding/refolding model of the VWF A2 domain and proteolysis by ADAMTS13. (A) Cartoon of the VWF A2 domain in its native folded state. (B) The first step of unfolding occurs from the C-terminal end of the VWF A2 domain, influenced by the presence of the vicinal disulphide bond (cysteines depicted by C). Initial unfolding occurs up to, or including, the central β4 sheet in which the scissile bond (YM) is contained. This unfolding intermediate step exposes the high-affinity ADAMTS13 spacer-binding site. (C) Once the stabilizing effect of the CBS is overcome this results in the complete unfolding of the VWF A2 domain and the positioning of the ADAMTS13 active site for nucleophilic attack of the Y1605-M1606 scissile bond.

length. Jakobi et al have directly linked the unfolding intermediate to the presence of Ca²⁺ and found that addition of EDTA reduced the frequency of its observation. Molecular dynamics simulations of force-induced unfolding have predicted that the VWF A2 domain unfolds from the C terminus, with a possible intermediate where $\alpha 6$, $\beta 6$, $\alpha 5$, $\beta 5$, and the $\alpha 4$ -less loop are peeled off, leaving the $\beta 4$ strand with the scissile bond and the rest of the N-terminal loops in a folded conformation that is compatible with Ca²⁺ binding.¹⁹ It should be noted that intermediates observed with the optical tweezers are not necessarily observed in solution thermal-unfolding experiments, and we have not detected a Ca²⁺-dependent intermediate, with our DSF curves in the main displaying fully cooperative unfolding.

Importantly, we provide here the first evidence for the protective role of Ca²⁺ occupancy of the CBS of the VWF A2 domain on the unfolding and susceptibility to cleavage by ADAMTS13 of FL-VWF. This protection is evident with or without the vicinal disulphide bond. We found that VWF with an intact CBS combined with the presence of the vicinal cysteines is highly resistant to proteolysis, as expected. Our results suggest that the stability provided by the interaction with Ca²⁺ needs to be overcome for subsequent proteolysis by ADAMTS13 and as such forms an important determinant in VWF A2 domain unfolding. Mutation of the vicinal cysteines, especially in combination with destabilizing D1498A and N1602A mutations of the Ca²⁺-binding site, greatly increased the proteolysis by ADAMTS13. In fact, VWF lacking both features may unfold spontaneously and sufficiently to allow ADAMTS13 cleavage without force-induced changes. The presence of the adjacent VWF domains in FL-VWF rescued the reduced expression and secretion of VWF A2 variants containing the mutated Ca²⁺-binding site and lacking the vicinal cysteines. Therefore, additional stability is conferred by variants in the context of FL-VWF. Nevertheless, the susceptibility of our FL-VWF variants to undergo proteolysis by ADAMTS13 generally reflected the stability of the isolated A2 domain variants in DSF assays. That the absence of both stabilizing Ca²⁺ binding and vicinal disulphide bond formation leads to proteolysis in the absence of urea further suggests that any modifications to both of these determinants of VWF A2 domain stability may have marked consequences on VWF multimer size and hemostatic function *in vivo*.

von Willebrand disease type 2A mutations are associated with a reduction in VWF multimer size.²⁰ Although some mutations affect intracellular VWF multimer formation, it has been shown with many mutations in the VWF A2 domain that there is an increase in susceptibility to proteolysis by ADAMTS13. Interestingly, the common R1597W mutation has been shown to affect the Ca²⁺-binding properties of the VWF A2 domain, thereby affecting the thermostability of the domain.¹⁸ Furthermore, the M1528V mutation which forms part of the hydrophobic pocket to which the vicinal disulphide bond interacts reduced the thermostability of the isolated VWF A2 domain but was still stabilized by the presence of Ca²⁺.¹⁸

We envisage that both the binding of Ca²⁺ and formation of the vicinal disulphide bond in the VWF A2 domain may be adversely influenced by clinical mutations such as in type 2A von Willebrand disease. It is conceivable also that changes in local Ca²⁺ concentration upon secretion, and reduction of the vicinal disulphide bond by oxidoreductases, could also adversely influence domain stability.

Taken together, our results in conjunction with previous studies on the interaction between ADAMTS13 and the VWF A2 domain⁴ lead us to propose a model for VWF A2 domain unfolding/refolding and proteolysis by ADAMTS13 (Figure 6). When tensile forces acting on the VWF are sufficient, VWF A2 domain unfolding begins from the C terminus and is heavily influenced by the presence of the vicinal disulphide bond. However, the stability conferred by this element is less than that provided by the CBS (compare T_m, see Table 1). When the stability provided by the vicinal disulphide bond is overcome this leads to partial unfolding to a possible unfolding intermediate of which the exact structure remains to be determined but that may incorporate the $\beta 4$ strand. The high affinity-binding site for the spacer domain of ADAMTS13 becomes exposed and we speculate that the interaction may influence the stability of the unfolding intermediate. Further unfolding of the VWF A2 domain is controlled by the coordination of the Ca²⁺ ion in the VWF A2 domain CBS. Disruption of Ca²⁺-coordinated interactions leads to further unfolding, or prevents refolding, and enables the positioning of the ADAMTS13 metalloprotease domain for the catalytic site to attack the scissile bond.

Acknowledgments

We are grateful to Dr Gareth Gerrard for the use of the Rotor Gene Q instrument.

This work was supported by a British Heart Foundation Basic Science Research Fellowship (grant FS/11/51/28920) and a grant from the National Institute for Health Research, Biomedical Research Centre Funding Scheme.

Authorship

Contribution: C.J.L., B.M.L., and D.A.L. designed the research; C.J.L. performed the experiments; and all authors analyzed the results and wrote the manuscript.

Conflict-of-interest disclosure: The authors declare no competing financial interests.

Correspondence: David A. Lane, Centre for Haematology, Imperial College London, Room 5.S5, Commonwealth Building, Hammersmith Hospital Campus, Du Cane Rd, London, W12 0NN, United Kingdom; e-mail: d.lane@imperial.ac.uk.

References

- Zhou Y-F, Eng ET, Zhu J, Lu C, Walz T, Springer TA. Sequence and structure relationships within von Willebrand factor. *Blood*. 2012;120(2):449-458.
- Sadler JE. Biochemistry and genetics of von Willebrand factor. *Annu Rev Biochem*. 1998;67:395-424.
- Zhang Q, Zhou Y-F, Zhang C-Z, Zhang X, Lu C, Springer TA. Structural specializations of A2, a force-sensing domain in the ultralarge vascular protein von Willebrand factor. *Proc Natl Acad Sci U S A*. 2009;106(23):9226-9231.
- Crawley JT, de Groot R, Xiang Y, Luken BM, Lane DA. Unraveling the scissile bond: how ADAMTS13 recognizes and cleaves von Willebrand factor. *Blood*. 2011;118(12):3212-3221.
- Jakobi AJ, Mashaghi A, Tans SJ, Huizinga EG. Calcium modulates force sensing by the von Willebrand factor A2 domain. *Nat Commun*. 2011;2:385.
- Zhou M, Dong X, Baldauf C, et al. A novel calcium-binding site of von Willebrand factor A2 domain regulates its cleavage by ADAMTS13. *Blood*. 2011;117(17):4623-4631.
- Tsai HM, Sussman II, Nagel RL. Shear stress enhances the proteolysis of von Willebrand factor in normal plasma. *Blood*. 1994;83(8):2171-2179.
- Zhang X, Halvorsen K, Zhang CZ, Wong WP, Springer TA. Mechanoenzymatic cleavage of the ultralarge vascular protein von Willebrand factor. *Science*. 2009;324(5932):1330-1334.
- Auton M, Cruz MA, Moake J. Conformational stability and domain unfolding of the von Willebrand factor A domains. *J Mol Biol*. 2007;366(3):986-1000.

10. Furlan M, Robles R, Lämmle B. Partial purification and characterization of a protease from human plasma cleaving von Willebrand factor to fragments produced by in vivo proteolysis. *Blood*. 1996;87(10):4223-4234.
11. Tsai HM. Physiologic cleavage of von Willebrand factor by a plasma protease is dependent on its conformation and requires calcium ion. *Blood*. 1996;87(10):4235-4244.
12. Marti T, Rösselet SJ, Titani K, Walsh KA. Identification of disulfide-bridged substructures within human von Willebrand factor. *Biochemistry*. 1987;26(25):8099-8109.
13. Luken BM, Winn LY, Emsley J, Lane DA, Crawley JT. The importance of vicinal cysteines, C1669 and C1670, for von Willebrand factor A2 domain function. *Blood*. 2010;115(23):4910-4913.
14. McKinnon TA, Chion AC, Millington AJ, Lane DA, Laffan MA. N-linked glycosylation of VWF modulates its interaction with ADAMTS13. *Blood*. 2008;111(6):3042-3049.
15. Xu AJ, Springer TA. Calcium stabilizes the von Willebrand factor A2 domain by promoting refolding. *Proc Natl Acad Sci U S A*. 2012; 109(10):3742-3747.
16. Niesen FH, Berglund H, Vedadi M. The use of differential scanning fluorimetry to detect ligand interactions that promote protein stability. *Nat Protoc*. 2007;2(9):2212-2221.
17. Michaux G, Hewlett LJ, Messenger SL, et al. Analysis of intracellular storage and regulated secretion of 3 von Willebrand disease-causing variants of von Willebrand factor. *Blood*. 2003; 102(7):2452-2458.
18. Xu AJ, Springer TA. Mechanisms by which von Willebrand disease mutations destabilize the A2 domain. *J Biol Chem*. 2013;288(9): 6317-6324.
19. Baldauf C, Schneppenheim R, Stacklies W, et al. Shear-induced unfolding activates von Willebrand factor A2 domain for proteolysis. *J Thromb Haemost*. 2009;7(12): 2096-2105.
20. Sadler JE, Budde U, Eikenboom JC, et al; Working Party on von Willebrand Disease Classification. Update on the pathophysiology and classification of von Willebrand disease: a report of the Subcommittee on von Willebrand Factor. *J Thromb Haemost*. 2006;4(10): 2103-2114.